

Rate constant for the generation of $^1\text{O}_2$ from commonly used triplet sensitizers: a systematic study of the wavelength effect using the ene reaction of 2,3-dimethyl-2-butene

Mamiko Hayakawa, Tadashi Aoyama, and Akihiko Ouchi*

Department of Materials and Applied Chemistry, College of Science and Technology, Nihon University
Kanda-Surugadai, Chiyoda-ku, Tokyo 101-8308, Japan
Email: ouchi.akihiko@nihon-u.ac.jp

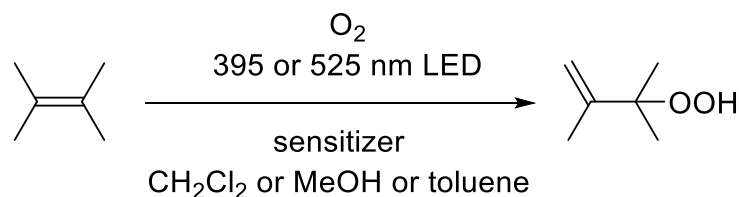
Received 09-29-2020

Accepted 11-16-2020

Published on line 11-29-2020

Abstract

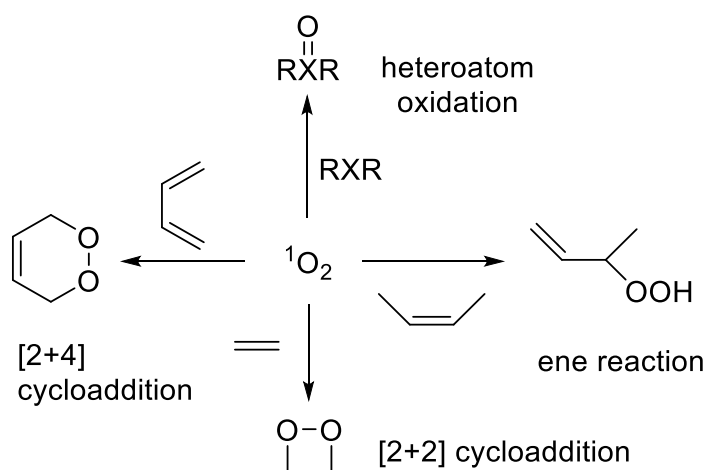
Singlet oxygen ($^1\text{O}_2$) has been widely used in organic synthesis to introduce oxygen-containing functional groups. It is usually generated from ground state oxygen via photochemical triplet sensitization using various organic dyes. To clarify the factors for increasing the efficiency of the reaction, we report a systematic determination of the rate constants observed for the generation of $^1\text{O}_2$ from commonly used triplet sensitizers, i.e., methylene blue, rose bengal, eosin Y, tetraphenylporphyrin, and C_{60} , using the ene reaction of 2,3-dimethyl-2-butene as a probe reaction utilizing 395 and 525 nm LEDs. A faster reaction was accomplished by the larger quantum yield for the generation of $^1\text{O}_2$, longer irradiation wavelength (λ), higher intensity of incident light (E), and larger $\varepsilon\lambda$ (the product of the irradiation wavelength λ and molar extinction coefficient at λ).



Keywords: Singlet oxygen, triplet sensitizer, ene reaction, efficiency, rate constant, wavelength effect

Introduction

Singlet oxygen ($^1\text{O}_2$, [$\text{O}_2(^1\Delta_g)$]) is an activated form of oxygen that is readily accessible from ground state oxygen found in air. It has been widely used toward the synthesis of organic compounds to introduce oxygen-containing functionalities, and its importance is increasing due to its small environmental impact during the course of its synthesis.¹ Since its discovery, extensive studies have been conducted and its fundamental reactions with organic compounds (ene reactions, [4+2] cycloadditions, [2+2] cycloadditions, heteroatom oxidations) (Scheme 1) have already been established in these early studies.²⁻⁴ After the initial stage of its study, the use of $^1\text{O}_2$ has been extended to the synthesis of complex organic molecules⁵⁻⁸ and many synthetic applications, and improvements have been developed^{3,9-16} together with its use in wastewater treatments¹⁷ and photodynamic therapy.¹⁸



Scheme 1. Singlet oxygen reactions.

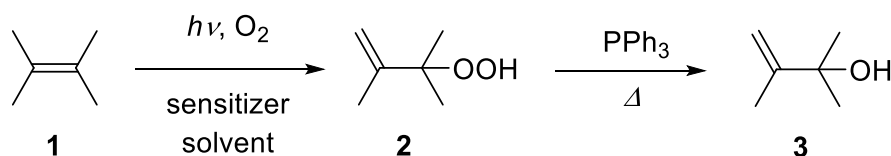
The most common method used for the generation of $^1\text{O}_2$ utilizes a photochemical process using triplet sensitizers.¹⁹⁻²³ Because of the different spin states of singlet oxygen, from ground state triplet oxygen, $^1\text{O}_2$ cannot be generated via the direct photochemical excitation of ground state oxygen. Thus, energy transfer from excited triplet sensitizers to ground state oxygen is generally used for the generation of $^1\text{O}_2$. Therefore, extensive studies on the physical properties of sensitizers, such as the quantum yield of their triplet state and $^1\text{O}_2$ formation, and their triplet energies and lifetimes, have been conducted using various techniques and standards.^{2-4,19-28} Various organic dyes have been used as triplet sensitizers in organic synthesis and their reactions proceed efficiently in many cases, although the irradiation time required varies from *hours* to *days*. Increasing the efficiency of the reaction is important for organic synthesis, not only by increasing the yield of the desired products but also by decreasing the reaction time. The selection of the solvent used has been reported to be important for determining the efficiency of the reaction via controlling the concentration of $^1\text{O}_2$ formed in the solution. However, besides the solvent, to the best of our knowledge, it is still not clear whether the difference in the efficiency only depends on the reactivity of the substrate with $^1\text{O}_2$, but also on the difference in the rate of $^1\text{O}_2$ generation.

As for investigations on the reactivity of the reaction substrates, the quenching rates of $^1\text{O}_2$ using various starting materials have been well studied.²⁹ On the other hand, as for the rate of $^1\text{O}_2$ generation, only a limited number of results have been reported. The relative rate has been reported for methylene blue (**MB**), rose bengal (**RB**), and eosin Y (**EY**) in water using the continuous emission of a Xe lamp with filters; the rates were

estimated from the development of nitroxide radicals using ESR measurements and the decomposition of deoxyguanosine using UV spectroscopy, which gave different relative rates for each sensitizer investigated.³⁰ The relative rate has also been reported for **MB**, **RB**, and **EY** in benzene/MeOH³¹ and MeOH³² using a 514.5 nm Ar laser and detecting $^1\text{O}_2$ using the emission observed at 1,268 nm. The rate constants have also been reported for tetraphenylporphyrin (**TPP**) and C_{60} in CCl_4 using a XeCl excimer laser (308 nm);³³ the authors claimed that their results were only valid in CCl_4 so that sensitizers insoluble in this solvent, such as **MB**, **RB**, and **EY**, have not been studied. However, some of these reported results on the rate of $^1\text{O}_2$ generation are not consistent with each other.

On the other hand, the irradiation wavelength is one of the important factors used to control photochemical reactions. The above results on the rate of $^1\text{O}_2$ generation were obtained using different light sources, which might be the reason for the inconsistency in the reported results. The quantum yield of $^1\text{O}_2$ generation is expected to be a factor for controlling the efficiency of $^1\text{O}_2$ reactions. The wavelength dependence on the quantum yield of $^1\text{O}_2$ generation has been reported for some porphyrins and metallo porphyrins,^{34–36} but other studies on the quantum yield of $^1\text{O}_2$ generation using various techniques and standards do not show any significant deviation in the reported values.^{26–28} The photodegradation of organic compounds by $^1\text{O}_2$ using a pyrrole derivative³⁷ and xanthene dyes³⁸ also exhibit wavelength dependence, but these photodegradation studies do not consider the difference in the molar extinction coefficients of the derivatives at the wavelength of irradiated light used. In contrast, the absence of wavelength dependence during the generation of $^1\text{O}_2$ has been reported for various furocoumarines and related molecules.³⁹ These results indicate that the presence of a wavelength dependence during the generation of $^1\text{O}_2$ for the commonly used triplet sensitizers is still not clear at the moment.

Therefore, a systematic study using the same method and substrate is necessary to clarify the factors for increasing the efficiency of the reaction, i.e. to determine the rate constants and obtain clear evidence for the presence or absence of a wavelength dependence during the generation of $^1\text{O}_2$ for commonly used triplet sensitizers. Herein, we report the determination of the rate constants of different sensitizers under the same conditions using the ene reaction of 2,3-dimethyl-2-butene (**1**) as a probe reaction (Scheme 2), utilizing 395 and 525 nm LEDs. The reaction of **1** \rightarrow **2** was reported to proceed almost quantitatively via triplet sensitized reactions^{40–44} and it has also been used as a probe reaction in kinetic studies on the generation of $^1\text{O}_2$ from the molybdenum-catalysed H_2O_2 reaction.⁴⁵ We have tested some widely used sensitizers, namely **MB**, **RB**, **EY**, **TPP**, and C_{60} , and determined their rate constants for the generation of $^1\text{O}_2$.



Scheme 2. The ene reaction of 2,3-dimethyl-2-butene (**1**) to give 3-hydroperoxy-2,3-dimethylbutene (**2**) and its reduction to 3-hydroxy-2,3-dimethylbutene (**3**).

Results and Discussion

UV absorption of various sensitizers

UV absorption spectra of the five sensitizers (**MB**, **RB**, **EY**, **TPP**, and **C₆₀**) and emission spectra of 395 and 525 nm LEDs are shown in Figure 1 and 2, respectively. Due to the solubility of the sensitizers, **MB**, **TPP**, and **C₆₀** were measured in CH₂Cl₂, and **MB**, **RB**, and **EY** in MeOH. **C₆₀** was also measured in toluene. Although the absorption maximum of **MB** was the same in CH₂Cl₂ and MeOH, and showed only a small difference between the two solvents, a red shift (6 nm) in the absorption maximum of **C₆₀** was observed in toluene when compared with that observed in CH₂Cl₂. Figure 1 shows the absorbance of **MB**, **EY**, and **RB** were 395 < 525 nm (corresponding to the emission of 395 and 525 nm LEDs), but those of **TPP** and **C₆₀** were 395 > 525 nm.

The absorption of **EY**, **RB**, and **MB** at 525 nm was attributed to the transition to their S₁ state and that at 395 nm to the absorption edge of their higher excited states. The emission of the 525 nm LED matched well with the absorption maximum of **EY**, but overlapped only at the absorption edge of **MB**. As for **TPP**, 525 nm light was absorbed by one of the Q bands and 395 nm light by the Soret band. As for **C₆₀**, the weak absorption at >430 nm corresponded to the orbital-forbidden electronic transitions and <430 nm to the allowed transitions.⁴⁶

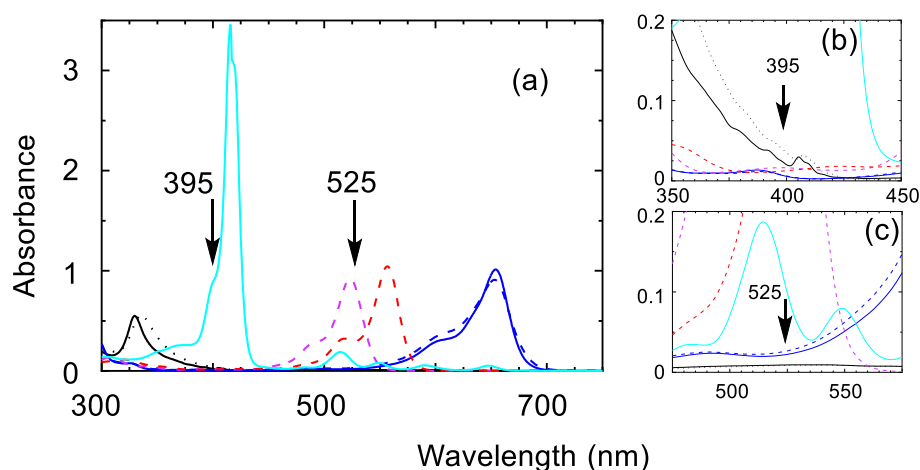


Figure 1. (a) UV absorption spectra of various sensitizers in different solvents. The wavelength at 395 and 525 nm are also shown in the figures. The concentration of the sensitizers was: (a) 1.00×10^{-5} M and (b, c) 1.00×10^{-4} M in CH₂Cl₂ (—), MeOH (---), and toluene (.....). Sensitizers: **MB**, blue; **EY**, violet; **RB**, red; **TPP**, light blue; **C₆₀**, black.

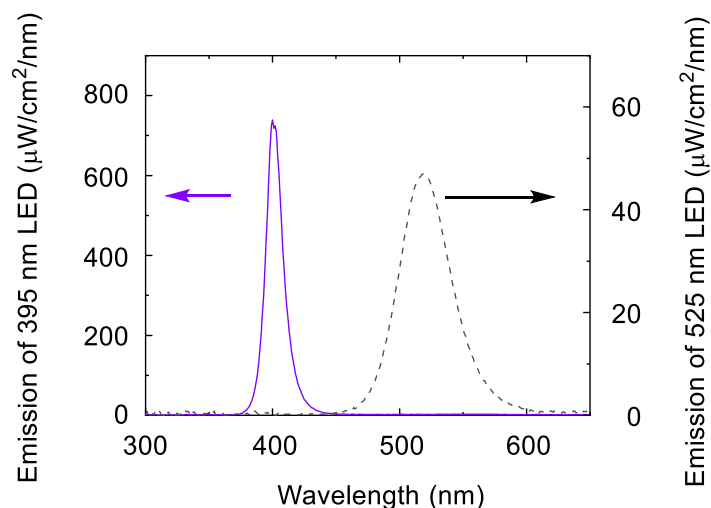


Figure 2. Emission spectra of 395 and 525 nm LEDs, measured 1.5 cm from the LED panels.

Ene reaction of 2,3-dimethyl-2-butene (**1**) using 395 and 525 nm LEDs

The results obtained from the ene reaction of **1** (30 mM, 10 mL) using the various sensitizers (0.12 mM) (Scheme 2) are shown in Figures 3 (395 nm LED) and 4 (525 nm LED). The reactions using **MB**, **TPP**, and **C₆₀** were conducted in CH_2Cl_2 (Figs. 3a–c and Figs. 4a,b), and those using **MB**, **RB**, and **EY** in MeOH (Figs. 3e–g and Figs. 4d–f). The reactions using **C₆₀** were also performed in toluene (Fig. 3d and Fig. 4c).

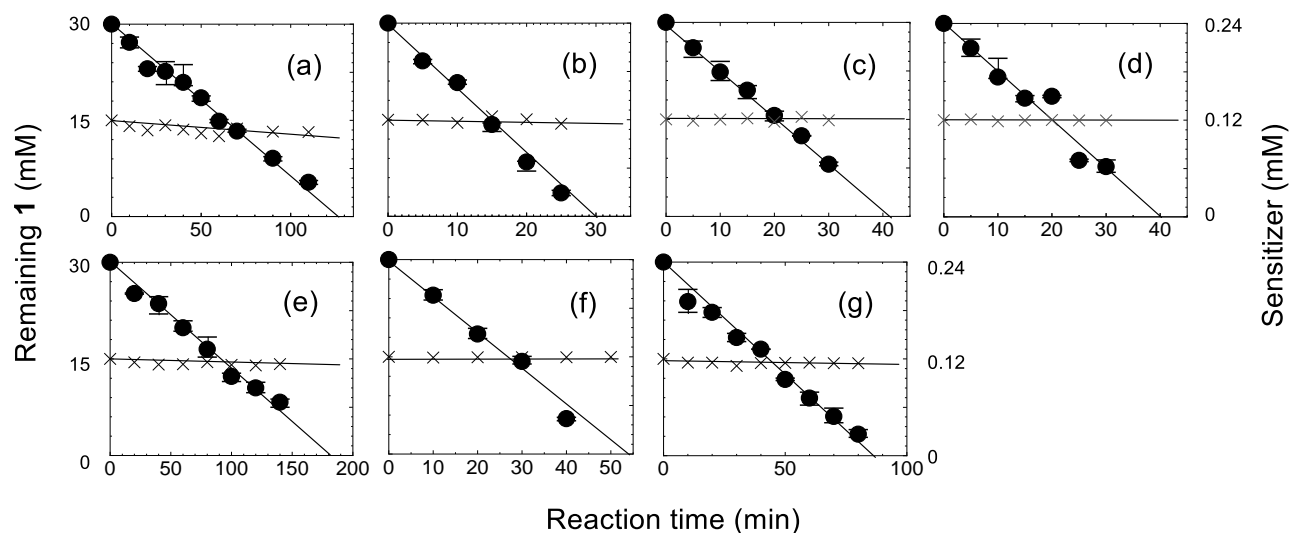


Figure 3. Ene reaction of 2,3-dimethyl-2-butene (**1**) using a 395 nm LED and various sensitizers. Symbols: **1** (•), sensitizer (×). Solvent: (a–c) CH_2Cl_2 , (d) toluene, (e–g) MeOH. Sensitizer: (a, e) **MB**, (b) **TPP**, (c, d) **C₆₀**, (f) **RB**, (g) **EY**. Photolysis condition: **1** (30 mM) and sensitizer (0.12 mM) in 10 mL solution; light source, 395 nm LED (13.36 mW/cm^2 , 370–475 nm, 1.5 cm from the LED panel); reaction vessel, quartz cylindrical cell (diameter: 3 cm); O_2 atmosphere; room temp.

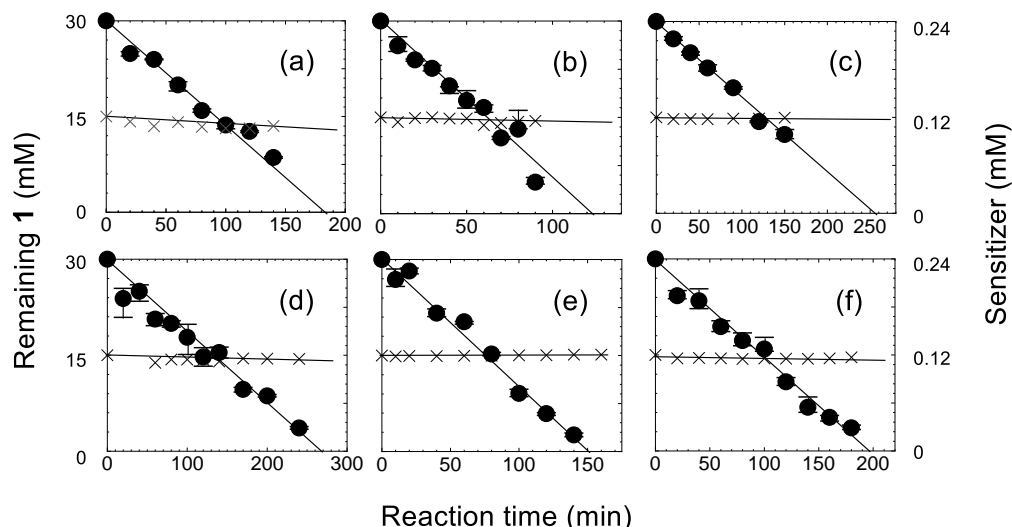


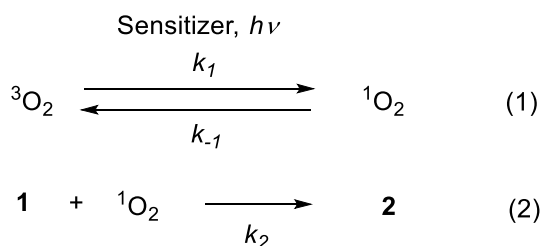
Figure 4. Ene reaction of 2,3-dimethyl-2-butene (**1**) using a 525 nm LED and various sensitizers. Symbols: **1** (●), sensitizer (×). Solvent: (a, b) CH₂Cl₂, (c) toluene, (d–f) MeOH. Sensitizer: (a, d) **MB**, (b) **TPP**, (c) **C₆₀**, (e) **RB**, (f) **EY**. Photolysis condition: **1** (30 mM) and sensitizer (0.12 mM) in 10 mL solution; light source, 525 nm LED (2.50 mW/cm², 455–620 nm, 1.5 cm from the LED panel); reaction vessel, quartz cylindrical cell (diameter: 3 cm); O₂ atmosphere; room temp.

As seen in the figures, a zero-order decay of starting material **1** was observed for all cases. The figures also showed that the decomposition of the sensitizers throughout the reaction was small. The results also showed a significant solvent effect in the reaction. As for **MB**, the reaction proceeded faster in CH₂Cl₂ than in MeOH (Fig. 3a vs 3e, and 4a vs 4d), which could be explained by the longer lifetime of ¹O₂ in CH₂Cl₂ (70–100 μs) than in MeOH (10.4 μs).^{26–28} In the case of **C₆₀**, the reaction did not show any significant difference between CH₂Cl₂ and toluene (Fig. 3d vs 3c).

Figures 3 and 4 show that the conversion of **1** proceeds faster under an 395 nm LED than the 525 nm LED, but it should be noted that the light intensity of the 395 nm LED (13.36 mW/cm²) was higher than that of the 525 nm LED (2.50 mW/cm²).

Rate constants and quantum yields for the generation of singlet oxygen for each sensitizer and wavelength studied

To compare the rate of ¹O₂ generation for each sensitizer, the rate constants were calculated for each sensitizer at an excitation wavelength of 395 and 525 nm, excluding the effects of the light intensity and molar absorption coefficient. Kinetic analysis was conducted using elementary reactions 1 and 2 shown in Scheme 3.



Scheme 3. Elementary reactions for the ene reaction of **1**.

Two kinetic equations (3 and 4) were derived from the two elementary reactions.

$$d[{}^1\text{O}_2]_t/dt = k_1 p [\text{sen}]_t [{}^3\text{O}_2]_t - k_2 [{}^1\text{O}_2]_t [\mathbf{1}]_t - k_{-1} [{}^1\text{O}_2]_t \quad (3)$$

$$- d[\mathbf{1}]_t/dt = k_2 [{}^1\text{O}_2]_t [\mathbf{1}]_t \quad (4)$$

where k_1 , k_{-1} , and k_2 are the rate constants for reactions 1 and 2, p is the number of photons absorbed by the sensitizer per unit time and sensitizer concentration,⁴⁷ and $[\mathbf{1}]_t$, $[\text{sen}]_t$, $[{}^3\text{O}_2]_t$, and $[{}^1\text{O}_2]_t$ are the concentrations of $\mathbf{1}$, sensitizer, ${}^3\text{O}_2$, and ${}^1\text{O}_2$ at time t , respectively. The reliable values of k_{-1} are reported to be $8.3 \times 10^4 - 1.1 \times 10^5$ (MeOH), $7.1 \times 10^3 - 1.9 \times 10^4$ (CH_2Cl_2), and $3.2 \times 10^4 - 5.0 \times 10^4$ (toluene) [s^{-1}],²⁹ and k_2 are $3 \times 10^7 - 4 \times 10^7$ (MeOH), $4 \times 10^7 - 5.2 \times 10^7$ (CH_2Cl_2), and $3.6 \times 10^7 - 4.2 \times 10^7$ (toluene) [Ms^{-1}].²⁹ As the initial concentration of $\mathbf{1}$ is 3.0×10^{-2} [M], the $k_2 [\mathbf{1}]_t$ values at $t = 0$ were calculated to be $9 \times 10^5 - 1.2 \times 10^6$ (MeOH), $1.2 \times 10^6 - 1.6 \times 10^6$ (CH_2Cl_2), $1.0 \times 10^6 - 1.3 \times 10^6$ (toluene) [s^{-1}] so that $k_2 [\mathbf{1}]_t \gg k_{-1}$ near $t = 0$. Therefore, equation 3 can be approximated as follows:

$$d[{}^1\text{O}_2]_t/dt = k_1 p [\text{sen}]_t [{}^3\text{O}_2]_t - k_2 [{}^1\text{O}_2]_t [\mathbf{1}]_t \quad (3')$$

during the initial stage of the reaction. As p , $[{}^3\text{O}_2]_t$ ($\approx [{}^3\text{O}_2]_s$, concentration of saturated ${}^3\text{O}_2$), and $[\text{sen}]_t$ ($\approx [\text{sen}]_0$ = 0.12 mM, initial concentration of the sensitizers) can be considered as constant, equation 5 can be derived from equation 3' and 4 using a steady state treatment.⁴⁷

$$[\mathbf{1}]_t = -k_1 p [\text{sen}]_0 [{}^3\text{O}_2]_s t + 3.0 \times 10^{-2} \quad (5)$$

The calculated and observed values for the reaction using 395 and 525 nm LEDs are listed in Table 1 and 2. The $p[\text{sen}]_0$ values were calculated from the molar absorption coefficients of the sensitizers and the intensity of light from the LEDs, in which the wavelength ranges used for the calculation were 370–475 nm for the 395 nm LED and 455–620 nm for the 525 nm LED.⁴⁷ The *reaction time* was determined at the intercept of the horizontal axes in Figure 3 and 4, which corresponded to the time required for the complete consumption of $\mathbf{1}$ when the initial stage of the reaction proceeded to completion. The p_{abs} value is defined by $p \times [\text{sen}]_0 \times \text{reaction time}$, which corresponded to the number of photons absorbed by the sensitizer for the complete consumption of $\mathbf{1}$. The quantum yields for the consumption of $\mathbf{1}$ (ϕ) were calculated to be 3×10^{-4} mol (initial amount of $\mathbf{1}$) / p_{abs} . However, the reaction of $\mathbf{1} \rightarrow \mathbf{2}$ proceeded almost quantitatively via the triplet sensitized reaction^{40–43} and the ϕ values were in good agreement with the quantum yields reported for ${}^1\text{O}_2$ generation by each sensitizer.^{4,23,26–28} Therefore, we can consider that the observed ϕ values were equal to the quantum yields of ${}^1\text{O}_2$ generation for each sensitizer. The $k_1 p[\text{sen}]_0 [{}^3\text{O}_2]_s$ values for each sensitizer were obtained from the slope of the decrease of $\mathbf{1}$ in Figure 3 and 4. The rate constant (k_1) values were obtained from $k_1 p [\text{sen}]_0 [{}^3\text{O}_2]_s$, $p [\text{sen}]_0$, and $[{}^3\text{O}_2]_s$, in which the $[\text{sen}]_0$ value was 0.12 M (concentration of sensitizer) and the $[{}^3\text{O}_2]_s$ values, the concentration of saturated ${}^3\text{O}_2$ in each solvent, were 10.2×10^{-3} (MeOH), 10.7×10^{-3} (CH_2Cl_2), and 9.88×10^{-3} (toluene) M.⁴⁸ Thus the obtained rate constants (k_1) were normalized in regards to the light intensity, molar absorption coefficient, and concentration of the sensitizer used.

Table 1. Rate constant (k_1) and quantum yield (ϕ) for the generation of $^1\text{O}_2$ using a 395 nm LED

Sensitizer	Solvent	$p[\text{sen}]_0$ (E min^{-1})	Reaction time (min)	p_{abs} (E)	ϕ	$k_1 p[\text{sen}]_0$ [$^3\text{O}_2$] _s (M min^{-1})	k_1 (E^{-1})
MB	MeOH	3.25×10^{-6}	190	6.18×10^{-4}	0.49	1.58×10^{-4}	4.76×10^3
EY		6.71×10^{-6}	86	5.77×10^{-4}	0.52	3.49×10^{-4}	5.10×10^3
RB		6.20×10^{-6}	54	3.35×10^{-4}	0.90	5.56×10^{-4}	8.78×10^3
MB	CH_2Cl_2	3.18×10^{-6}	126	4.00×10^{-4}	0.75	2.38×10^{-4}	7.01×10^3
TPP		10.69×10^{-6}	30	3.21×10^{-4}	0.94	10.00×10^{-4}	8.75×10^3
C ₆₀		7.67×10^{-6}	41	3.15×10^{-4}	0.95	7.32×10^{-4}	8.92×10^3
C ₆₀	Toluene	7.72×10^{-6}	40	3.09×10^{-4}	0.97	7.50×10^{-4}	9.83×10^3

[$^3\text{O}_2$]_s = 10.2 (MeOH), 10.7 (CH_2Cl_2), 9.88 (toluene) mM,⁴⁸ E = mol-photons.

Photolysis condition: intensity of light, 13.36 mW/cm^2 ; wavelength range, 370–475 nm; [**1**]₀ = 30 mM; [sen]₀ = 0.12 mM; solution: 10 mL.

Table 2. Rate constant (k_1) and quantum yield (ϕ) for the generation of $^1\text{O}_2$ using a 525 nm LED

Sensitizer	Solvent	$p[\text{sen}]_0$ (E min^{-1})	Reaction time (min)	p_{abs} (E)	ϕ	$k_1 p[\text{sen}]_0$ [$^3\text{O}_2$] _s (M min^{-1})	k_1 (E^{-1})
MB	MeOH	2.20×10^{-6}	268	5.89×10^{-4}	0.51	1.12×10^{-4}	4.99×10^3
EY		2.42×10^{-6}	195	4.71×10^{-4}	0.64	1.54×10^{-4}	6.25×10^3
RB		2.57×10^{-6}	150	3.85×10^{-4}	0.78	2.00×10^{-4}	7.63×10^3
MB	CH_2Cl_2	1.96×10^{-6}	182	3.56×10^{-4}	0.84	1.65×10^{-4}	7.88×10^3
TPP		2.47×10^{-6}	123	3.03×10^{-4}	0.99	2.44×10^{-4}	9.24×10^3
C ₆₀	Toluene	1.18×10^{-6}	256	3.02×10^{-4}	0.99	1.17×10^{-4}	10.06×10^3

[$^3\text{O}_2$]_s = 10.2 (MeOH), 10.7 (CH_2Cl_2), 9.88 (toluene) mM,⁴⁸ E = mol-photons.

Photolysis condition: intensity of light, 2.50 mW/cm^2 ; wavelength range, 455–620 nm; [**1**]₀ = 30 mM; [sen]₀ = 0.12 mM; solution: 10 mL.

As seen in Table 1 and 2, a wavelength effect on the quantum yield was observed for **EY** and **RB** in MeOH and **MB** in CH_2Cl_2 , but this effect was not seen for **MB** in MeOH and **TPP** in CH_2Cl_2 , which indicated that the wavelength effect was dependent on the solvent used; a solvent effect on the quantum yield of $^1\text{O}_2$ generation has been reported for Mg and Zn tetrabenzoporphyrins.³⁵ In the case of **RB** in MeOH, a larger quantum yield was obtained using the shorter wavelength of irradiation, which was attributed to the presence of intersystem crossing from the higher singlet excited state(s).³⁵

The wavelength effect was also observed in the rate constants for the generation of $^1\text{O}_2$. Table 3 shows the relative rate constants (k_1) for each sensitizer. For both 395 and 525 nm LED irradiation, the k_1 values were in the order of: **MB** < **EY** < **RB** (MeOH), which was consistent with the reported relative rate obtained using an Ar ion laser (514.5 nm) [**EY** < **RB** (MeOH)],³² but the order of **MB** was different in the other solvent system **EY** < **RB** < **MB** (benzene/MeOH).³¹ However, another study on the relative rate using continuous emission of a Xe

lamp by monitoring the generation of $^1\text{O}_2$ by decomposition of deoxyguanosine showed the order of the generation of $^1\text{O}_2$ was **MB** < **EY** < **RB** (H_2O), which is consistent with our results.²⁹

Table 3 Relative rate constant for the generation of $^1\text{O}_2$

Solvent	Sensitizer	Relative k_1	
		395 nm LED	525 nm LED
MeOH	MB	1.00	1.00
	EY	1.07	1.25
	RB	1.84	1.53
CH_2Cl_2	MB	1.00	1.00
	TPP	1.25	1.17
	C_{60}	1.27	-

We have observed the wavelength dependence on the quantum yield and that the wavelength effect was dependent on the solvent used. Therefore, the inconsistency in the order of the relative rate observed for the different sensitizers between the reported studies^{30–32} and our results could be explained by the different solvents and wavelengths of irradiated light used in each of the experiments.

Figure 5 shows the correlation between the rate constants (k_1) and quantum yields for $^1\text{O}_2$ generation. As shown in the figure, the rate constant was proportional to the quantum yield, irrespective of the utilized triplet sensitizer, solvent, or wavelength of irradiated light used. Therefore, the selection of sensitizers with a large quantum yield for the generation of $^1\text{O}_2$ was necessary for the larger k_1 value. On the other hand, equation 5 indicated that larger p , $[\text{sen}]_0$, and $[\text{}^3\text{O}_2]_s$ values were responsible for faster reactions. As for $[\text{sen}]_0$, it was suggested that a sensitizer concentration of $2 \times 10^{-4} - 2 \times 10^{-3}$ M resulted in a good balance between maximizing the absorption of photons and avoiding the inner filter effects.⁴ The selection of solvents having higher saturated oxygen concentration ($[\text{}^3\text{O}_2]_s$) values was preferable. As $p \propto \lambda$, E , $(1 - 10^{-a\epsilon\lambda})$ (a : constant),⁴⁷ longer irradiation wavelength (λ), higher intensity of incident light (E), and larger $\epsilon\lambda$ (the product of irradiation wavelength λ and molar extinction coefficient at λ) were required for faster reactions. The parameters indicated above were all affected by the solvent and wavelength of irradiated light used.

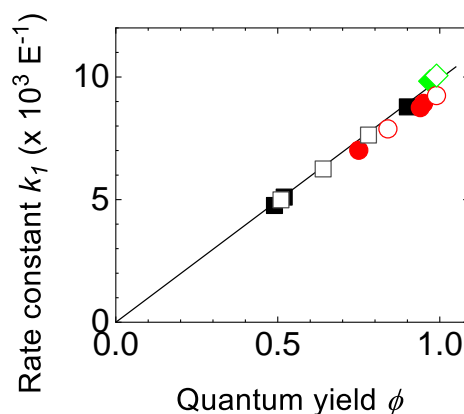


Figure 5. Correlation between the rate constant and quantum yield for $^1\text{O}_2$ generation. Solvent: MeOH (\blacksquare, \square), CH_2Cl_2 (\bullet, \circ), toluene (\blacklozenge, \lozenge). Light source: 395 nm LED ($\blacksquare, \bullet, \blacklozenge$), 525 nm LED (\square, \circ, \lozenge).

Conclusions

To clarify the factors for increasing the efficiency of the reaction, a systematic study determining the rate constant for the generation of $^1\text{O}_2$ using common triplet sensitizers, i.e., methylene blue (**MB**), rose bengal (**RB**), eosin Y (**EY**), tetraphenylporphyrin (**TPP**), and C_{60} , has been conducted using the ene reaction of 2,3-dimethyl-2-butene (**1**) as a probe reaction. The wavelength effect was investigated using 395 and 525 nm LEDs. The rate constants and the quantum yields for the generation of $^1\text{O}_2$ observed for the sensitizers showed both the presence and absence of the wavelength effect, which depended on the solvent used. The wavelength effect on the quantum yield was observed for **EY** and **RB** in MeOH and **MB** in CH_2Cl_2 , but not for **MB** in MeOH and **TPP** in CH_2Cl_2 . The order of the rate constant was **MB** < **EY** < **RB** (MeOH) and **MB** < **TPP** < C_{60} (CH_2Cl_2) for both 395 and 525 nm LEDs. A faster reaction was accomplished by the larger quantum yield for the generation of $^1\text{O}_2$, longer irradiation wavelength (λ), higher intensity of incident light (E), and larger $\varepsilon\lambda$ (the product of the irradiation wavelength λ and molar extinction coefficient at λ), which were all affected by the solvent and wavelength of irradiated light used.

Experimental Section

General. ^1H NMR (400 MHz) and ^{13}C NMR (100 MHz) spectra were recorded with a JEOL ECX 400 spectrometer using CDCl_3 as solvent. As internal standards, TMS (δ 0.0 ppm) was used for ^1H NMR, and CDCl_3 (δ 77.0 ppm) for ^{13}C NMR analyses. UV measurements were conducted by using a Shimadzu UV-2400PC UV-vis spectrophotometer. GC analyses were performed by using a Shimadzu GC-2014 capillary GLC (INERT CAP1, 60 m, 0.25 mmID, $df = 0.25\ \mu\text{m}$, GL Sciences Inc.) fitted with a flame-ionization detector. Emission spectra and intensity of the LEDs were measured with an Ushio Spectral Radiometer USR-40D.

2,3-Dimethyl-2-butene (**1**) ($\geq 99\%$, SIGMA-ALDRICH), triphenylphosphine (min. 98.0%, Kanto Chemical), dichloromethane (for spectroscopy, Kanto Chemical), methanol (for fluorometry, Kanto Chemical), toluene (for spectroscopy, Kanto Chemical), methylene blue (ion association reagent for spectrometric analysis, TCI), rose bengal ($>98.0\%$, TCI), eosin Y (guaranteed reagent grade, Wako Pure Chemical), TPP (ultrahigh sensitive spectrophotometric reagent for Cu, TCI), and C_{60} (99.5+%, MTR) were purchased and used as bought. 3-Hydroxy-2,3-dimethyl-2-butene (**3**) was synthesized according to the reported procedure.⁴⁹

General procedure for the photolysis. A solution (10 mL) of 2,3-dimethyl-2-butene (**1**) (30 mM, 0.3 mmol) and sensitizer (0.12 mM) was introduced into a quartz cylindrical cell (diameter: 3 cm) fitted with a three-way stopcock. The solution was degassed and replaced with oxygen using three vacuum-sonication- O_2 purging cycles.⁵⁰ The photolysis were conducted using a 395 or 525 nm LED (IZUMI Opto Device) under an oxygen atmosphere. The emission spectra and its intensity were measured on a Ushio Spectral Radiometer USR-40D. After the photolysis, the amount of remaining sensitizer was determined using UV spectrometry with a 1-mm optical path cell. The reaction mixture was stirred a further 2 h in the dark under an air atmosphere after the addition of PPh_3 (0.6 mmol), and the remaining **1** in the reaction mixture were then determined using glc analysis.

Acknowledgements

This work was supported by Nihon University College of Science and Technology Grants-in-Aid B. We thank Ms. Tomoka Asaga and Mr. Taku Kamimura for preliminary experiments.

Supplementary Material

[1] Derivation of eq 5 from eqs 3' and 4, and [2] number of photons absorbed by the solution per unit time.

References and Notes

1. Ravelli, D.; Protti, S.; Neri, P.; Fagnoni, M.; Albini, A. *Green Chem.* **2011**, *13*, 1876–1884.
<https://doi.org/10.1039/c0gc00507j>
2. Frimer, A. H. In *The Chemistry of Functional Groups, Peroxides*; Patai S. Ed.; John Wiley & Sons: Chichester, 1983; pp. 201–234, Chapter 7.
3. Stratakis, M.; Orfanopoulos, M. *Tetrahedron* **2000**, *56*, 1595–15.
[https://doi.org/10.1016/S0040-4020\(99\)00950-3](https://doi.org/10.1016/S0040-4020(99)00950-3)
4. Clennan, E. L. In *Singlet Oxygen*; Nonell, S.; Flors C. Eds.; Royal Society of Chemistry: Cambridge, 2016; Vol. 1, pp. 353–367, Chapter 18.
5. Montagnon, T.; Tofi, M.; Vassilikogiannakis, G. *Accounts Chem. Res.* **2008**, *41*, 1001–1011.
<https://doi.org/10.1021/ar800023v>
6. Iesce, M. R.; Cermola, F. In *CRC Handbook of Organic Photochemistry and Photobiology*, 3rd. Ed; Griesbeck, A. G.; Oelgemöller, M.; Ghatti F. Eds.; CRC Press: Boca Raton, 2012; Vol. 1, Chapter 30.
7. Ghogare, A. A.; Greer, A. *Chem. Rev.* **2016**, *116*, 9994–10034.
<https://doi.org/10.1021/acs.chemrev.5b00726>
8. Griesbeck, A. G.; Sillner, S.; Kleczka, M. In *Singlet Oxygen*; Nonell, S.; Flors C. Eds.; Royal Society of Chemistry: Cambridge, 2016; Vol. 1, pp. 369–392, Chapter 19.
9. Griesbeck, A. G.; El-Idreesy, T. T.; Lex, J. *Tetrahedron* **2006**, *62*, 10615–10622.
<https://doi.org/10.1016/j.tet.2006.05.093>
10. Alberti, M. N.; Vassilikogiannakis, Orfanopoulos, M. *Org. Lett.* **2008**, *10*, 3997–4000.
<https://doi.org/10.1021/ol801488w>
11. Zamadar, M.; Greer, A. In *Handbook of Synthetic Photochemistry*; Albini, A.; Fagnoni M. Eds.; Wiley-VCH: Weinheim, 2010; pp. 353–386, Chapter 11.
12. Alberti, M. N.; Orfanopoulos, M. In *CRC Handbook of Organic Photochemistry and Photobiology*, 3rd. Ed; Griesbeck, A. G.; Oelgemöller, M.; Ghatti F. Eds.; CRC Press: Boca Raton, 2012; Vol. 1, Chapter 31.
13. Lamb, B. M.; Barbas III, C. F. *Chem. Commun.*, **2015**, *51*, 3196–3199.
<https://doi.org/10.1039/C4CC09040C>
14. Okada, A.; Nagasawa, Y.; Yamaguchi, T.; Yamaguchi, E.; Tada, N.; Miura, T.; Itoh, A. *RSC Adv.* **2016**, *6*, 42596–42599.
<https://doi.org/10.1039/C6RA07084A>

15. Kalaizakis, D.; Triantafyllakis, M.; Ioannou, G. I.; Vassilikogiannakis, G. *Angew. Chem. Int. Ed.* **2017**, *56*, 4020–4023. And references cited therein.
<https://doi.org/10.1002/anie.201700620>
16. Deng, J.; Gui, J. *Synlett* **2019**, *30*, 642–646.
<https://doi.org/10.1055/s-0037-1611943>
17. García, N. A.; Pajares, A. M.; Bregliani, M. M. In *Singlet Oxygen*; Nonell, S.; Flors C. Eds.; Royal Society of Chemistry: Cambridge, 2016; Vol. 1, pp. 447–457, Chapter 23.
18. Luby, B. M.; Walsh, C. D.; Zheng, G. *Angew. Chem. Int. Ed.* **2019**, *58*, 2558–2569.
<https://doi.org/10.1002/anie.201805246>
19. Ogilby, P. R.; Foote, C. S. *J. Am. Chem. Soc.* **1983**, *105*, 3423–3430.
<https://doi.org/10.1021/ja00349a007>
20. Arbogast, J. W.; Darmanyan, A. P.; Foote, C. S.; Rubin, Y.; Diederich, F. N.; Alvarez, M. M.; Anz, S. J.; Whetten, R. L. *J. Phys. Chem.* **1991**, *95*, 11–12.
<https://doi.org/10.1021/j100154a006>
21. DeRosa, M. C.; Crutchley, R. J. *Coord. Chem. Rev.* **2002**, *233–234*, 351–371.
[https://doi.org/10.1016/S0010-8545\(02\)00034-6](https://doi.org/10.1016/S0010-8545(02)00034-6)
22. Schmidt, R. *Photochem. Photobiol.* **2006**, *82*, 1161–1177.
<https://doi.org/10.1562/2006-03-03-IR-833>
23. Fresnadillo, D. G.; Lacombe, S. In *Singlet Oxygen*; Nonell, S.; Flors C. Eds.; Royal Society of Chemistry: Cambridge, 2016; Vol. 1, pp. 105–143, Chapter 6.
24. Kearns, D. R. *Chem. Rev.* **1971**, *71*, 395–427.
<https://doi.org/10.1021/cr60272a004>
25. Schweitzer, C.; Schmidt, R. *Chem. Rev.* **2003**, *103*, 1685–1757.
<https://doi.org/10.1021/cr010371d>
26. Gorman, A. A.; Rodgers, M. A. J. In *CRC Handbook of Organic Photochemistry*, Vol. II, Chapter 10, Scaiano, J. C. Ed., CRC Press: Boca Raton, 1989.
27. Wilkinson, F.; Helman, W. P.; Ross, A. B. *J. Phys. Chem. Ref. Data* **1993**, *22*, 113–262, Table 2.
<https://doi.org/10.1063/1.555934>
28. Redmond, R. W.; Gamlin, J. N. *Photochem. Photobiol.* **1999**, *70*, 391–475.
<https://doi.org/10.1111/j.1751-1097.1999.tb08240.x>
29. Wilkinson, F.; Helman, W. P.; Ross, A. B. *J. Phys. Chem. Ref. Data* **1995**, *24*, 663–1021, Table 1 and 2.
<https://doi.org/10.1063/1.555965>
30. Houba-Herlin, N.; Calberg-Bacq, C. M.; Piette, J.; Van de Vorst, A. *Photochem. Photobiol.* **1982**, *36*, 297–306.
<https://doi.org/10.1111/j.1751-1097.1982.tb04378.x>
31. Nagano, T.; Arakane, K.; Ryu, A.; Masunaga, T.; Shinmoto, K.; Mashiko, S.; Hirobe, M. *Chem. Pharm. Bull.* **1994**, *42*, 2291–2294.
<https://doi.org/10.1248/cpb.42.2291>
32. Arakane, K.; Ryu, A.; Takarada, K.; Masunaga, T.; Shinmoto, K.; Kobayashi, R.; Mashiko, S.; Nagano, T.; Hirobe, M. *Chem. Pharm. Bull.* **1996**, *44*, 1–4.
<https://doi.org/10.1248/cpb.44.1>
33. Schweitzer, C.; Mehrdad, Z.; Noll, A.; Grabner, E.-W.; Schmidt, R. *J. Phys. Chem. A* **2003**, *107*, 2192–2198.
<https://doi.org/10.1021/jp026189d>
34. Bennett, L. E.; Ghigginio, K. P.; Henderson, R. W. *J. Photochem. Photobiol. B: Biol.* **1989**, *3*, 81–89.

35. Lavi, A.; Johnson, F. M.; Ehrenberg, B. *Chem. Phys. Lett.* **1994**, 231, 144–150.
[https://doi.org/10.1016/0009-2614\(94\)01262-8](https://doi.org/10.1016/0009-2614(94)01262-8)
36. Starukhin, A.; Knyukshto, V.; Plavskii, V.; Gorski, A.; Solariski, J. *EPJ Web of Conference* **2017**, 132, 02019.
<https://doi.org/10.1051/epjconf/201713202019>
37. Mizuno, T.; Hanamori, M.; Akimoto, K.; Nakagawa, H.; Arakawa, K. *Chem. Pharm. Bull.* **1994**, 42, 160–162.
<https://doi.org/10.1248/cpb.42.160>
38. Goda, Y.; Sato, K.; Hori, N.; Takeda, M.; Maitani, T. *Chem. Pharm. Bull.* **1994**, 42, 1510–1513.
<https://doi.org/10.1248/cpb.42.1510>
39. Jones, S. G.; Young, A. R.; Truscott, T. G. *J. Photochem. Photobiol. B: Biol.* **1993**, 21, 223–227.
[https://doi.org/10.1016/1011-1344\(93\)80187-E](https://doi.org/10.1016/1011-1344(93)80187-E)
40. Fuchter, M. J.; Hoffman, B. M.; Barrett, A. G. M. *J. Org. Chem.* **2006**, 71, 724–729.
<https://doi.org/10.1021/jo052156t>
41. Hino, T.; Anzai, T.; Kuramoto, N. *Tetrahedron Lett.* **2006**, 47, 1429–1432.
<https://doi.org/10.1016/j.tetlet.2005.12.081>
42. Han, X.; Bourne, R. A.; Poliakoff, M.; George, M. W. *Green Chem.* **2009**, 11, 1787–1792.
<https://doi.org/10.1039/b914074c>
43. Murthy, R. S.; Bio, M.; You, Y. *Tetrahedron Lett.* **2009**, 50, 1041–1044.
<https://doi.org/10.1016/j.tetlet.2008.12.069>
44. Camussi, I.; Mannucci, B.; Speltini, A.; Profumo, A.; Milanese, C.; Malavasi, L.; Quadrelli, P. *ACS Sustain. Chem. Eng.* **2019**, 7, 8176–8182.
<https://doi.org/10.1021/acssuschemeng.8b06164>
45. Sels, B. F.; De Vos, D. E.; Jacobs, P. A. *J. Am. Chem. Soc.* **2007**, 129, 6916–6926.
<https://doi.org/10.1021/ja065849f>
46. Leach, S.; Vervloet, M.; Desprès, A.; Bréheret, E.; Hare, J. P.; Dennis, T. J.; Kroto, H. W.; Taylor, R.; Walton, D. R. M. *Chem. Phys.* **1992**, 160, 451–466.
[https://doi.org/10.1016/0301-0104\(92\)80012-K](https://doi.org/10.1016/0301-0104(92)80012-K)
47. See Supplementary materials 1 and 2.
48. Montalti, M.; Credi, A.; Prodi, L.; Gandolfi, M. T. *Handbook of Photochemistry, Third Edition*; CRC Press: Boca Raton, 2006; Chapter 9, Table 9c.
<https://doi.org/10.1201/9781420015195>
49. Kraft, P.; Popaj, K. *Eur. J. Org. Chem.* **2004**, 4995–5002.
<https://doi.org/10.1002/ejoc.200400577>
50. Ouchi, A.; Liu, C.; Kaneda, M.; Hyugano, T. *Eur. J. Org. Chem.* **2013**, 3807–3816.
<https://doi.org/10.1002/ejoc.201300115>

This paper is an open access article distributed under the terms of the Creative Commons Attribution (CC BY) license (<http://creativecommons.org/licenses/by/4.0/>)